Title

Signature of supernova neutrino flavor mixing in water Čerenkov detectors

Journal

Physical Review D, 49(4)

ISSN

2470-0010

Authors

Qian, Yong-Zhong
Fuller, George M

Publication Date

1994-02-15

DOI

10.1103/physrevd.49.1762

Peer reviewed

Signature of supernova neutrino flavor mixing in water Čerenkov detectors

Yong-Zhong Qian and George M. Fuller
Department of Physics, 0319, University of California, San Diego, 9500 Gilman Dr., La Jolla, California 92093-0319
(Received 8 September 1993)

We study supernova neutrino burst signals in large water Čerenkov detectors, examining the effects of mixing between ν_e and either ν_μ or ν_τ, and taking account of charged current ν_e capture on oxygen in the detector. We show that the characteristic count rates and angular distributions from supernova neutrino-induced events can depend sensitively on the degree of neutrino flavor mixing. This sensitivity results from the different average energies expected in supernova models for ν_e on the one hand and ν_μ and ν_τ on the other, the steep increase in the $^{16}\mathrm{O}(\nu_e,e^-)^{16}\mathrm{F}$ cross section with neutrino energy, and the backward-peaked nature of the exit channel electron in this reaction. Neutrino flavor-mixing effects would be identifiable in the super Kamiokande detector for the neutrino burst of a galactic supernova.

PACS number(s): 95.55.Vj, 14.60.Pq, 95.85.Ry, 97.60.Bw

I. INTRODUCTION

In this paper we study the effects of neutrino flavor mixing on the detection of a supernova neutrino burst event. Some previous studies have concentrated on how neutrino flavor mixing might alter the type-II supernova explosion mechanism [1,2]. Other work has involved analyses of the SN 1987A neutrino signals to constrain neutrino flavor mixing [3,4]. Neutrino oscillations in supernovas in general are discussed in Ref. [5].

The SN 1987A case has been discussed extensively following the detection of its neutrinos by the Kamiokande II (KII) and IMB detectors [6]. Only 11 and 8 neutrino-induced events were detected by the KII and IMB detectors, respectively. These data cannot provide any reliable information about neutrino flavor mixing without specific, and questionable, assumptions being made. Most of the neutrino-induced events in these detectors are expected to be from $\bar{\nu}_e+p\rightarrow n+e^+$. If the vacuum masses for neutrinos obey $m_{\nu_{\tau(\mu)}}>m_{\nu_e}$, then there will be no matter-enhancement effects in supernovas for $\bar{\nu}_e\rightleftharpoons\bar{\nu}_{\tau(\mu)}$ oscillations. However, since the first event detected in the KII detector was forward peaked, there was speculation that it originated from scattering ($\nu_e+e^-\rightarrow\nu_e+e^-$). Attempts to constrain neutrino flavor mixing in SN 1987A centered around this single event [3,4]. These attempts were based on two assumptions. These assumptions were that (1) the first event was due to $\nu_e e^-$ scattering and (2) the ν_e originated in the "neutronization pulse."

Haxton [7] has subsequently pointed out that electron-neutrino capture by oxygen in water Čerenkov detectors can have an important impact on the detection of high energy neutrinos. In turn, this reaction makes the characteristics of the neutrino-induced events in water Čerenkov detectors sensitive to mixing between lower average energy ν_e and higher average energy ν_μ and ν_τ. In fact, the sensitivity of the $^{16}\mathrm{O}(\nu_e,e^-)^{16}\mathrm{F}$ induced event rate to neutrino energy will allow us to show that neutrino flavor mixing has a readily detectable signature in the super Kamiokande (SK) water Čerenkov detector for a galactic supernova.

We first discuss some aspects of neutrino emission from supernovas. It is fashionable to consider three distinct phases of neutrino emission associated with type-II supernovas: the infall pulse, the neutronization pulse, and the thermal emission phase [8]. In actuality, numerical calculations show that these phases are not really completely distinct [9]. High energy ν_e from electron capture reactions are emitted during the infall phase of collapse. The neutronization pulse occurs when the shock passes through the "neutrino sphere." The thermal emission phase corresponds to the cooling and deleptonization of the hot protoneutron star. In this final phase, the gravitational binding energy of the nascent neutron star is radiated away nearly equally in ν_e, $\bar{\nu}_e$, ν_μ, $\bar{\nu}_\mu$, ν_τ, and $\bar{\nu}_\tau$.

In the thermal emission phase, each neutrino species has approximately a blackbody-type spectrum (Fermi-Dirac, zero chemical potential). These neutrino spectra can be characterized by the temperature of the neutrino sphere for each species. In this study, we assume that neutrinos are emitted from one single neutrino sphere, even though neutrinos of different energies decouple at slightly different radii. The $\nu_\mu(\bar{\nu}_\mu)$ and $\nu_\tau(\bar{\nu}_\tau)$ have identical spectra. The corresponding average energies for these species are considerably higher than those for ν_e and $\bar{\nu}_e$. This is because the ν_μ and ν_τ have lower opacities than do $\nu_e(\bar{\nu}_e)$ and, hence, decouple deeper in the core [9]. The temperatures which characterize these neutrino distributions generally satisfy $T_{\nu_{\tau(\mu)}}>T_{\bar{\nu}_e}>T_{\nu_e}$. Numerical calculations show considerable evolution in the neutrino temperatures with time. Early in the thermal emission phase, before there has been significant deleptonization of the surface layers of the neutron star, the ν_e and $\bar{\nu}_e$ temperatures are comparable, $T_{\bar{\nu}_e}\approx T_{\nu_e}$. Later, when this surface region is deleptonized and neutron rich, the $\bar{\nu}_e$ and ν_e temperatures satisfy $T_{\bar{\nu}_e}>T_{\nu_e}$ [9].

For our subsequent discussion of the effects of neutrino flavor mixing on supernova neutrino burst detection, we will adopt $T_{\nu_e}=T_{\bar{\nu}_e}=5$ MeV and $T_{\nu_x}=T_{\bar{\nu}_x}=7$ MeV ($x=\mu$ or τ). In what follows, we compare the event rates

for $\bar{\nu}_e + p \rightarrow n + e^+$ and $^{16}O(\nu_e, e^-)^{16}F$ in water Čerenkov detectors. In gauging the effects of $\nu_{\tau(\mu)} \rightleftharpoons \nu_e$ oscillations, our assumptions about characteristic neutrino temperatures are conservative. In fact, we will tend to overestimate the $^{16}O(\nu_e, e^-)^{16}F$ rate without oscillations by assuming $T_{\nu_e} = T_{\bar{\nu}_e}$ and underestimate the enhancement in this rate with $\nu_{\tau(\mu)} \rightleftharpoons \nu_e$ transformations by taking $T_{\nu_e} = 7$ MeV. At late times, numerical calculations show that T_{ν_x} might even be larger than 7 MeV [9].

Since the neutrino energy emitted in the neutronization pulse is a few percent of that emitted in the thermal emission phase, the majority of the neutrino events in the detectors comes from the latter. The presence of comparable numbers of neutrinos of each flavor in the thermal emission phase makes the neutrino flavor-mixing problem more complicated. Our main concern in this paper will be the neutrinos from the thermal emission phase.

In the following sections, we will examine the effects of $\nu_{\tau(\mu)} \rightleftharpoons \nu_e$ transformations on the expected supernova neutrino signal in water Čerenkov detectors. We will not consider the effects of transformations among the antineutrinos here. In Sec. II we discuss neutrino-induced events in water Čerenkov detectors. Neutrino oscillations in supernovas are examined in Sec. III. The changes in the expected supernova neutrino signal from neutrino oscillations are studied in Sec. IV. Conclusions are presented in Sec. V.

II. NEUTRINO-INDUCED EVENTS IN WATER ČERENKOV DETECTORS

In this paper, when we refer to "water Čerenkov detectors," we mean detectors such as KII and IMB. Although both the KII and IMB detectors have stopped operating, they unambiguously detected the neutrinos from SN 1987A. It is also our purpose in this paper to show that not much information about neutrino flavor mixing can be obtained from the detection of SN 1987A neutrinos. Furthermore, the detector characteristics of KII and IMB are well known in the literature. Therefore we will use these two detectors as examples to study supernova neutrino signals in water Čerenkov detectors. This study is relevant because KII is being upgraded to SK with a better detection efficiency and a much larger fiducial mass of water.

The main contribution to the total neutrino signal in these detectors comes from $\bar{\nu}_e$ absorption on protons: $\bar{\nu}_e + p \rightarrow n + e^+$. The angular distribution of the final state positrons from this reaction is nearly isotropic. This is because the $\bar{\nu}_e$ energies are always low compared to the nucleon mass. With considerations of neutron recoil and forbidden effects of the same order, the actual distribution is slightly backward peaked. This angular distribution is

$$P(\phi) \approx 0.5 - 0.051 \cos\phi \ , \tag{1}$$

where ϕ is the angle between the incoming $\bar{\nu}_e$ and the outgoing positron [10].

Neutrino-electron scattering can make some contribution to the total supernova neutrino signal in a water Čerenkov detector. In general, we expect the distribution of the scattered electrons in the detector to be strongly forward peaked. From kinematics, the angle between the incoming neutrino and the recoil electron satisfies $\cos\phi > \sqrt{U/(U+2)}$, where U is the electron recoil kinetic energy in terms of the electron rest mass energy. Since the detection threshold energies exceed 5 MeV in both the KII and IMB detectors, we can conclude that $\cos\phi > 0.91$. The $\nu_e e^-$ scattering cross section is larger by about a factor of 6 than the $\nu_\mu e^-$ or $\nu_\tau e^-$ scattering cross sections, since the $\nu_e e^-$ channel has a charged current contribution which the others lack. Note also that the $\nu_e e^-$ scattering cross section is larger than that for $\bar{\nu}_e e^-$ scattering. Therefore we expect that most scattering events in water Čerenkov detectors will result from $\nu_e e^-$ scattering.

As pointed out by Haxton [7], electron-neutrino absorption on natural oxygen can become important for water Čerenkov detectors. This process will make a larger contribution to the overall neutrino signal in a water Čerenkov detector than will $\nu_e e^-$ scattering whenever $T_{\nu_e} > 5$ MeV. Although Haxton has considered both the $^{16}O(\nu_e, e^-)^{16}F$ and $^{18}O(\nu_e, e^-)^{18}F$ reactions, the former makes the dominant contribution to the total ν_e absorption rate in water Čerenkov detectors. This is because ^{16}O is the predominant naturally occurring isotope of oxygen. Like the angular distribution of positrons from $\bar{\nu}_e$ absorption on protons, the distribution of electrons for $^{16}O(\nu_e, e^-)^{16}F$ is somewhat backward peaked. However, the electron angular distribution for $^{16}O(\nu_e, e^-)^{16}F$ depends on the ν_e energy. The harder the ν_e energy spectrum is, the stronger the backward-peaked tendency will be. From Fig. 2 given in Ref. [7], we find that for $T_{\nu_e} = 5$ MeV the electron angular distribution is given by

$$P(\phi) \approx 0.492 - 0.394 \cos\phi + 0.024 \cos^2\phi \tag{2a}$$

for the KII detector and

$$P(\phi) \approx 0.493 - 0.407 \cos\phi + 0.021 \cos^2\phi \tag{2b}$$

for the IMB detector. For $T_{\nu_e} = 7$ MeV, the electron angular distribution becomes

$$P(\phi) \approx 0.508 - 0.399 \cos\phi - 0.024 \cos^2\phi \tag{3a}$$

for the KII detector and

$$P(\phi) \approx 0.510 - 0.406 \cos\phi - 0.030 \cos^2\phi \tag{3b}$$

for the IMB detector. In this paper, we calculate the effective cross sections for neutrino-electron scattering for the KII and IMB detectors and take other cross sections from Table I given in Ref. [7]. These cross sections are listed in Table I for two representative neutrino temperatures.

We think that two other issues are worth mentioning here. One is the role of inelastic neutral current scattering of neutrinos on oxygen, and the other is the role of ν_e absorption on oxygen in the Sudbury Neutrino Observatory (SNO) detector.

The working mechanism for the water Čerenkov detectors such as KII, IMB, and even SK is to record the

TABLE I. Effective cross section $\sigma_{\rm eff}$ for neutrino interaction processes. These cross sections are in units of 10^{-42} cm^2. Numbers in the upper two rows are for the KII detector, and those in the lower ones are for the IMB detector.

T (MeV)	$p(\bar{\nu}_e,e^+)n$	$O(\bar{\nu}_e,e^+)N$	$\bar{\nu}_e e^- \to \bar{\nu}_e e^-$	$\bar{\nu}_x e^- \to \bar{\nu}_x e^-$	$\nu_x e^- \to \nu_x e^-$	$\nu_e e^- \to \nu_e e^-$	$O(\nu_e,e^-)F$
5	52.9	0.609	0.195		0.120	0.785	0.829
7				0.167	0.208	1.34	5.63
5	17.8	0.213	0.0181		0.0153	0.105	0.297
7				0.0339	0.0442	0.303	3.31

Čerenkov radiation from the electrons or positrons after the neutrino interaction event. Inelastic neutral current scattering of neutrinos on oxygen produces no electrons or positrons in the final state. The protons or neutrons knocked out of the oxygen nuclei are not detectable in the conventional water Čerenkov detectors. And neither are the γ rays radiated from the deexcitation of the excited oxygen nuclei. Therefore these neutral current processes are not a central issue in water Čerenkov detectors. And they provide no information about neutrino flavor mixing.

As for the SNO detector, it is very different in that it uses heavy water (D_2O) in addition to light water (H_2O). The charged current neutrino interactions on deuterium, which make more significant contributions to the total event rate than similar interactions on oxygen, also produce backward-peaked electrons or positrons [5]. Therefore the role of ν_e absorption on oxygen in the SNO detector is minor, and information about neutrino flavor mixing can be extracted from other neutrino interaction processes.

III. NEUTRINO FLAVOR MIXING IN SUPERNOVAS

The neutrino spectrum expected at a detector on Earth from a supernova neutrino burst event will in general depend on whether or not neutrinos have mass. Massive neutrinos can cause time-of-flight modifications in the neutrino signal at the detector (see Ref. [5]), or the neutrino energy spectrum could be modified by matter-enhanced $\nu_e \rightleftharpoons \nu_x$ transformations resulting from ν_e-ν_μ and/or ν_e-ν_τ neutrino mass level crossings in supernovas.

We do not know if neutrinos have mass. Currently, experiments can only provide upper limits on vacuum neutrino masses. These limits are generous enough to encourage speculation among astrophysicists and cosmologists. Two astrophysical puzzles suggest interesting and plausible mass ranges for ν_μ and ν_τ: the solar neutrino problem and the dark matter problem.

The matter-enhanced $\nu_e \rightleftharpoons \nu_x$ transformation can provide a convenient solution to the solar neutrino problem [11]. The most likely solution is the nonadiabatic transformation scenario, in which $\delta m^2 \sin^2 2\theta \approx 4\times 10^{-8}$ eV^2 for $\delta m^2 = 10^{-7}$–10^{-5} eV^2, where $\delta m^2 = m_2^2 - m_1^2$ is the difference of the squares of the vacuum neutrino masses and θ is the vacuum mixing angle [11]. Recent results from the GALLEX experiment [12] narrow the range of δm^2 to 3×10^{-6}–10^{-5} eV^2. Theoretical particle physics models of neutrino masses can be constructed in which either ν_e-ν_μ or ν_e-ν_τ mixing provides the appropriate level crossing in the Sun [13,14].

A ν_μ or ν_τ with a mass in the range of 1–100 eV could provide a component of the missing mass in the Universe. The Cosmic Background Explorer (COBE) discovery of a net quadrupole moment in the cosmic microwave background radiation distribution has been interpreted as suggesting a need for neutrinos with vacuum masses of a few eV [15]. Some theoretical particle physics models of neutrino masses can accommodate a ν_e-ν_μ level crossing in the Sun (i.e., $m_{\nu_\mu} \sim 10^{-3}$ eV) with a cosmologically significant ν_τ (i.e., $m_{\nu_\tau} \sim 1$ eV) [13,14]. Although these considerations are suggestive, there is no definitive evidence for neutrino mass to be obtained from astrophysics.

If we assume that the vacuum neutrino masses obey $m_{\nu_{\tau(\mu)}} > m_{\nu_e}$, then ν_e-ν_μ and/or ν_e-ν_τ level crossings could occur in supernovas. In this case, we expect a neutrino mass level crossing above the neutrino sphere whenever $m_{\nu_{\tau(\mu)}} \leq 100$ eV. Interestingly, neutrino flavor mixing in the supernova environment potentially can probe the neutrino mass range of interest in both the solar neutrino problem and the dark matter problem [2,16].

Since ν_μ and ν_τ have identical energy spectra, a ν_e-ν_μ or ν_e-ν_τ level crossing at a given radius produces the same effects on the detected supernova neutrino spectrum. For vacuum neutrino masses obeying $m_{\nu_\tau} > m_{\nu_\mu} > m_{\nu_e}$, it is possible to get sequential level crossings: ν_e-ν_τ followed by ν_e-ν_μ. In what follows, we study this double level crossing case. We will take as examples cases where vacuum neutrino masses satisfy $\delta m^2 \approx 1$–10^4 eV^2 for ν_e-ν_τ level crossings and $\delta m^2 \approx 3\times 10^{-6}$–$10^{-5}$ eV^2 for ν_e-ν_μ level crossings. This will serve to illustrate the effects of neutrino flavor mixing on supernova neutrino burst detection. In fact, with either one or two level crossings, for any vacuum neutrino mass satisfying $m_{\nu_{\tau(\mu)}} \leq 100$ eV, the resulting effects on the supernova neutrino signal will be broadly similar to those derived in our example cases. A schematic picture of the positions of level crossings in supernovas for our example cases is shown in Fig. 1. In this figure, the "mantle" refers to regions of the supernova which were influenced by hydrostatic presupernova nuclear burning, while "envelope" refers to the presupernova hydrogen envelope.

A ν_e propagating through the supernova environment above the neutrino sphere will acquire an effective mass from interactions with matter. The effective mass for ν_e

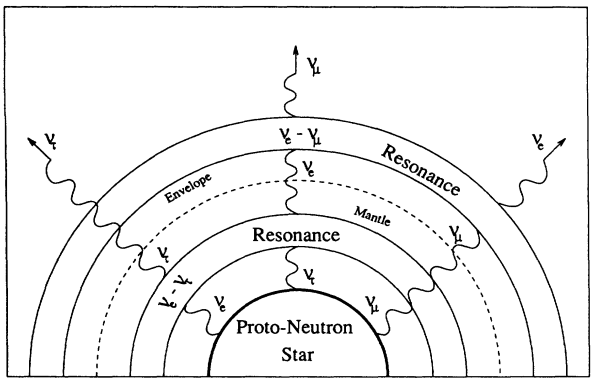

FIG. 1. Illustration of neutrino flavor mixing in supernovas.

will be larger than that for $\nu_\tau(\nu_\mu)$ due to charged current $\nu_e e^-$ forward scattering. A neutrino mass level crossing, or resonance, occurs when the difference of the squares of the vacuum neutrino mass eigenvalues, δm^2, and the vacuum mixing angle θ satisfy

$$\frac{\delta m^2}{2E_\nu}\cos 2\theta \approx \sqrt{2} G_F n_e \ , \tag{4}$$

where E_ν is the energy of the propagating neutrino, G_F is the Fermi constant, and $n_e = \rho N_A Y_e$ is the net electron number density ($n_e = n_{e^-} - n_{e^+}$), with ρ the matter density in $\mathrm{g\,cm^{-3}}$, N_A Avogadro's number, and Y_e the net number of electrons per baryon. In this expression we neglect neutrino-neutrino scattering contributions to the effective weak potential seen by the propagating neutrino. This approximation is justified in Refs. [16] and [17].

For small vacuum mixing angles ($\theta \ll 1$), we can employ the Landau-Zener approximation to estimate the probability that a ν_e propagating into the resonance region emerges as a ν_e [18]. This probability is

$$P_{\nu_e \to \nu_e} \approx \exp\{-\pi H \delta m^2 \sin^2 2\theta / 4E_\nu\} \ , \tag{5}$$

where $H = |d \ln\rho/dr|^{-1}_{\mathrm{res}}$ is the density scale height in the supernovas at the position of the resonance. In the case where a ν_e-ν_τ level crossing is followed by a ν_e-ν_μ level crossing, we can write the probability for a ν_e emitted from the neutrino sphere to arrive at a detector on Earth in the same flavor state as [4]

$$P_{\nu_e \to \nu_e} \approx \exp\{-\pi (H_{12} \delta m^2_{12} \sin^2 2\theta_{e\mu} + H_{13} \delta m^2_{13} \sin^2 2\theta_{e\tau}) / 4E_\nu\} \ . \tag{6}$$

In this expression, H_{12} and H_{13} are the density scale heights at the positions of the ν_e-ν_μ and ν_e-ν_τ resonances, respectively. The vacuum mixing angles $\theta_{e\mu}$ and $\theta_{e\tau}$ refer to ν_e-ν_μ and ν_e-ν_τ mixings, respectively.

Very little is known about the vacuum mixing angles $\theta_{e\mu}$ and $\theta_{e\tau}$. Laboratory neutrino oscillation experiments provide only neutrino-mass-dependent upper limits on these quantities [19]. Mixing angles consistent with these limits could effect large-scale matter-enhanced $\nu_e \rightleftharpoons \nu_\tau$ and/or $\nu_e \rightleftharpoons \nu_\mu$ interconversion in supernovas for extensive ranges of ν_μ and ν_τ vacuum masses [2,16].

In this paper, we will adopt values of δm^2_{12}, δm^2_{13}, $\theta_{e\mu}$, and $\theta_{e\tau}$, which result in a fair amount of $\nu_e \rightleftharpoons \nu_x$ conversion in supernovas, but which are consistent with experimental constraints, astrophysical limits, and the cherished hopes of some researchers. In fact, the signature of neutrino flavor mixing which we identify is not dependent on the details of these choices. In our calculation, we consider two representative values for δm^2_{12}: 4×10^{-6} and 8×10^{-6} eV^2. We also study two representative

TABLE II. Density scale height $|d \ln\rho/dr|^{-1}$ at resonance. Values of $|d \ln\rho/dr|^{-1}$ in the first two columns are for resonance in the envelope, those in the two middle columns are for resonance in the mantle at TPB=0.177 s, and those in the last two columns are for resonance in the mantle at TPB=0.638 s.

δm^2 (eV^2)	4×10^{-6}	8×10^{-6}	225	3600	225	3600
E (MeV)	$\times10^{10}$ (cm)	$\times10^{10}$ (cm)	$\times10^{6}$ (cm)	10^{6} (cm)	$\times10^{5}$ (cm)	$\times10^{5}$ (cm)
2	1.074	0.852	4.083	1.013	2.04	0.4906
2.828	1.094	1.070	3.06	1.11	2.61	0.815
3.999	0.992	1.074	6.84	0.787	2.71	0.576
5.654	1.008	1.094	6.94	1.509	4.19	1.324
7.995	1.062	0.992	7.1	1.89	4.88	0.936
11.31	1.061	1.008	10.8	2.412	3.45	2.52
15.99	0.815	1.062	15.7	2.91	4.53	3.20
22.60	0.497	1.061	14.9	3.07	6.53	2.89
31.96	1.023	0.815	19.87	4.33	4.62	2.041
45.19	1.958	0.497	11.7	4.37	7.354	2.62
63.90	2.167	1.023	8.27	4.66	9.83	2.72
90.36	2.541	1.958	7.6	6.95	6.96	4.194
127.8	3.516	2.167	5.38	7.11	14.4	4.88
180.7	4.269	2.541	3.8	10.85	10.21	3.453
255.5	4.217	3.516	12.8	11.07	37.0	4.537
361.2	5.565	4.269	9.03	14.9	28.6	6.53

values for δm^2_{13}: 225 and 3600 eV^2. For $\sin^2 2\theta_{e\mu}$ we adopt the "nonadiabatic" solution to the solar neutrino problem, $\sin^2 2\theta_{e\mu} \approx 4\times 10^{-6}$ eV$^2/\delta m^2_{12}$, while for $\sin^2 2\theta_{e\tau}$, we adopt $\sin^2 2\theta_{e\tau} \approx 4\times 10^{-6}$. The mixing angle $\theta_{e\tau}$ is chosen to be consistent with r-process nucleosynthesis in the hot bubble region of supernovas [16]. With these choices for δm^2 and $\sin^2 2\theta$, we will generally have sequential neutrino mass level crossings for ν_e-ν_τ and ν_e-ν_μ mixings. Were this not the case and, for example, we had only one resonance region, our results would not change enough to alter the conclusions regarding the expected signature of neutrino flavor mixing in water detectors.

Another ingredient in estimates of neutrino flavor conversion in supernovas is the density profile of the material above the neutrino sphere to be expected during the time of significant neutrino cooling. Conceivably, we need the density profiles for the entire star for times up to the order of the time post core bounce (TPB) ≈ 10 s. However, the KII and IMB detector observations for SN 1987A show that 70% of the neutrino-induced events were detected in the first 2 s. The density profile of the material in the envelope is nearly static over the period of interest. For the region close to the neutrino sphere (the "mantle"), the density profile also seems to maintain a nearly time-independent shape. In fact, this shape follows from the nearly hydrostatic conditions expected for TPB ~ 1 s. Numerical calculations show that most of the time dependence of the density profile in this region at this epoch comes from the decrease in the radius of the neutron star [16]. This does affect the conversion probabilities in Eq. (6), but in a manner which is easy to calculate, since the density profile remains roughly self-similar during this slow evolution.

We study neutrino flavor mixing at two representative epochs (TPB ≈ 0.177 s and TPB ≈ 0.638 s) with the Mayle-Wilson supernova density profiles [2,16,20]. We expect broadly similar results for calculations based on other supernova models. The density scale heights employed in our calculations for level crossings corresponding to our adopted values of δm^2_{12} and δm^2_{13} and a range of neutrino energies are presented in Table II.

IV. CALCULATION OF NEUTRINO-INDUCED EVENTS IN WATER ČERENKOV DETECTORS

In the absence of neutrino flavor mixing, the number of neutrino-induced events expected from each individual neutrino interaction process in the detector is given by

$$N_i(\text{event}) = N_{\text{H}_2\text{O}} \Phi_{\nu_i} (\sigma_{\text{eff}})_i \ , \tag{7}$$

where $N_{\text{H}_2\text{O}}$ is the number of water molecules in the detector, Φ_{ν_i} is the appropriate neutrino flux, and $(\sigma_{\text{eff}})_i$ is the effective cross section for the individual neutrino interaction process. The neutrino flux is approximately given by

$$\Phi_{\nu_i} \approx \frac{E_B/6}{\langle E_{\nu_i} \rangle} \frac{1}{4\pi D^2} \approx 2.758\times 10^{11} \text{ cm}^{-2} \left[\frac{E_B}{10^{53} \text{ erg}} \right] \left[\frac{\text{MeV}}{T_{\nu_i}} \right] \left[\frac{10 \text{ kpc}}{D} \right]^2 , \tag{8}$$

where E_B is the gravitational binding energy of the nascent neutron star (assumed to be radiated in the thermal emission phase), $\langle E_{\nu_i} \rangle$ is the average neutrino energy ($\langle E_{\nu_i} \rangle \approx 3.152 T_{\nu_i}$ for the neutrino energy spectra we have assumed), and D is the distance to the supernova. The effective cross section is defined as

$$(\sigma_{\text{eff}})_i = n_i \int f_{\nu_i} dE_{\nu_i} \int \epsilon \, d\sigma_i \ , \tag{9}$$

where n_i is the number of targets for the individual neutrino interaction process in one water molecule ($n_i = 10$ for neutrino-electron scattering, $n_i = 2$ for $\bar{\nu}_e$ absorption on protons, and $n_i = 1$ for ν_e capture on oxygen), f_{ν_i} is the neutrino energy spectrum, ϵ is the electron or positron detection efficiency of the detector, and $d\sigma_i$ is the energy differential cross section [$d\sigma_i \equiv (d\sigma_i/dE_e) dE_e$, where E_e is the electron or positron energy]. The neutrino energy spectrum is taken to be

$$f_{\nu_i} \approx \frac{1}{1.803} \frac{1}{T^3_{\nu_i}} \frac{E^2_{\nu_i}}{\exp(E_{\nu_i}/T_{\nu_i}) + 1} \ , \tag{10}$$

and the electron or positron detection efficiency is approximately

$$\epsilon \approx 1 - \exp[-(E_e/E_{\text{th}})^p] \ ,$$

where $E_{\text{th}} \approx 9$ MeV and $p \approx 3.0$ for the KII detector and $E_{\text{th}} \approx 34$ MeV and $p \approx 3.1$ for the IMB detector [7]. Hence we can write

$$N_i(\text{event}) \approx 9.219 \left[\frac{E_B}{10^{53} \text{ erg}} \right] \left[\frac{10 \text{ kpc}}{D} \right]^2 \left[\frac{M_{\text{H}_2\text{O}}}{\text{kton}} \right] \left[\frac{\text{MeV}}{T_{\nu_i}} \right] \left[\frac{(\sigma_{\text{eff}})_i}{10^{-42} \text{ cm}^2} \right] , \tag{11}$$

where M_{H_2O} is the mass of water in the detector, which is 2.14 and 6.8 kton for the KII and IMB detectors, respectively. With the assumption that $T_{\nu_e}=T_{\bar{\nu}_e}=5$ MeV, $T_{\nu_x}=T_{\bar{\nu}_x}=7$ MeV $(x=\mu,\tau)$, $E_B\approx 2\times 10^{53}$ erg, and $D\approx 10$ kpc, we compute and present the expected number of events corresponding to each individual neutrino interaction process in Table III. In this table, we give event totals for $\bar{\nu}_e$ absorption, neutrino-electron scattering, and ν_e capture on oxygen. These totals are given for the case of no neutrino flavor transformation in the rows labeled by $P_{\nu_e\to\nu_e}=1$.

With neutrino flavor mixing, the number of neutrino-electron scattering induced events and $^{16}O(\nu_e,e^-)^{16}F$ induced events will change. The increase in the number of neutrino-electron scattering induced events is given by

$$\delta N(\nu+e)\approx N_e\int (F^0_{\nu_x}-F^0_{\nu_e})(1-P_{\nu_e\to\nu_e})dE_\nu \times\int \epsilon[d\sigma(\nu_e+e)-d\sigma(\nu_x+e)]\ , \quad (12)$$

where N_e is the number of electrons in the detector and $F^0_{\nu_i}=\Phi_{\nu_i}f_{\nu_i}$. The increase in the number of $^{16}O(\nu_e,e^-)^{16}F$ induced events is given by

$$\delta N(\nu_e+O)=N_{H_2O}\int (F^0_{\nu_x}-F^0_{\nu_e})(1-P_{\nu_e\to\nu_e})dE_\nu \times\int \epsilon\, d\sigma(\nu_e+O)\ . \quad (13)$$

Even in the most favorable case of full conversion ($P_{\nu_e\to\nu_e}=0$), the net increase in the total number of scattering induced events due to neutrino flavor mixing is small, being about $\delta N(\nu+e)=1$ and 2 for the KII and IMB detectors, respectively. This small change due to neutrino flavor transformation is a result of compensating changes in the neutrino-electron scattering cross sections and the neutrino fluxes. In fact, the neutrino-electron scattering cross sections increase approximately linearly with neutrino energy, whereas the neutrino fluxes reaching the detector scale roughly inversely with the individual average neutrino energies.

By contrast, the cross section for $^{16}O(\nu_e,e^-)^{16}F$ induced events increases rapidly with neutrino energy. In fact, the cross section becomes very large only for neutrino energies greater than the effective threshold energy of $E_\nu\sim 35$ MeV. This corresponds to an excitation energy in ^{16}O where significant forbidden weak strength channels open up [7,21]. The enhanced energy dependence in the cross section can more than compensate for the reduction in neutrino flux due to neutrino flavor mixing. This situation is illustrated in Fig. 2, where the relative contributions of individual neutrino interaction processes to the neutrino-induced events in the KII and IMB detectors are shown as functions of neutrino temperature. The relative contributions of neutrino interaction processes are

TABLE III. Expected number of neutrino-induced events in the KII and IMB detectors. $P_{\nu_e\to\nu_e}=1$ refers to the case without neutrino oscillation, and $P_{\nu_e\to\nu_e}=0$ means full conversion of ν_e into $\nu_{\pi(\mu)}$. Numbers in the upper two rows are for the KII detector, and those in the lower ones are for the IMB detector.

$P_{\nu_e\to\nu_e}$	$\bar{\nu}_e$ absorption	$e\nu\to e'\nu'$	$O(\nu_e,e^-)F$	Total
1	422	12	7	441
0	422	13	32	467
1	451	6	7	464
0	451	8	59	518

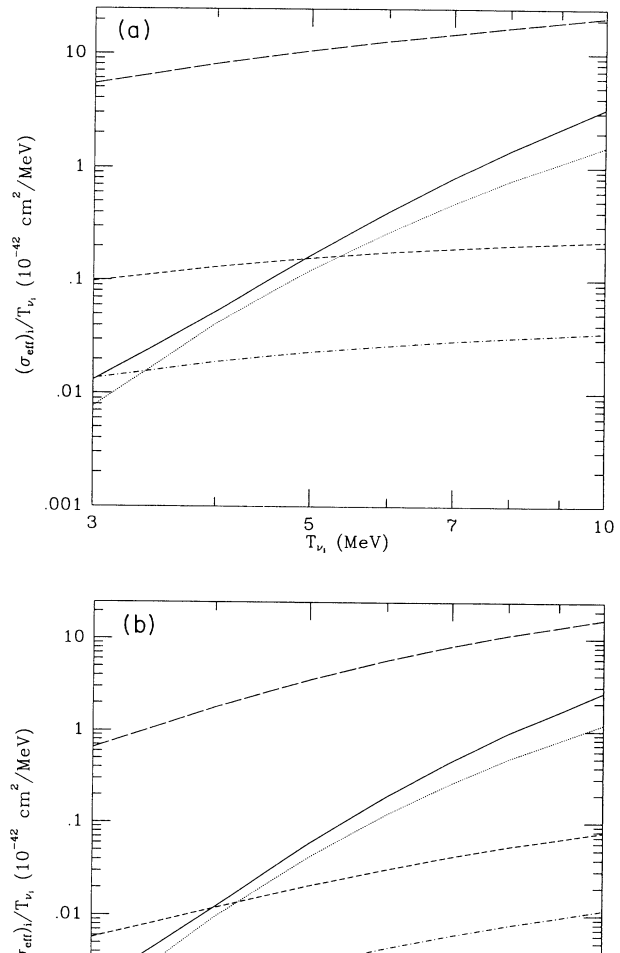

FIG. 2. Relative contributions of individual neutrino interaction processes to the neutrino-induced events in water Čerenkov detectors as functions of neutrino temperature. The solid line is for $O(\nu_e,e^-)F$, the dotted line is for $O(\bar{\nu}_e,e^+)F$, the short-dashed line is for $\nu_e e^-$ scattering, the long-dashed line is for $p(\bar{\nu}_e,e^+)n$, and the dot–short-dashed line is for $\nu_x e^-$ $(x=\mu$ or $\tau)$ scattering. (a) is for events in the KII detector, and (b) is for events in the IMB detector.

best gauged by comparing the ratio of effective cross section to neutrino temperature, $(\sigma_{\rm eff})_i/T_{\nu_i}$. This ratio is plotted in Figs. 2(a) and 2(b) for the KII and IMB detectors, respectively.

From Fig. 1 in Ref. [7], we find that the largest contribution to the $^{16}{\rm O}(\nu_e,e^-)^{16}{\rm F}$ induced events in the detectors comes from ν_e with energies around $E_{\nu_e}\approx 7.19T_{\nu_e}$. This result follows on assuming the energy spectrum in Eq. (10). Substantial conversion between ν_e and ν_x corresponds to the value of $P_{\nu_e\to\nu_e}$ being small. As a rough criterion for finding detectable event rate changes from neutrino flavor mixing, we find that we must have a conversion probability $P_{\nu_e\to\nu_e}\le e^{-1}$ for $E_{\nu_e}\approx 50$ MeV. The scale heights turn out to be $H_{12}\sim 10^{10}$ cm for ν_e-ν_μ resonance and $H_{13}\sim 10^6$ cm for ν_e-ν_τ resonance for the mixing parameters adopted above [2,16,20]. For these scale heights, our conversion criterion is satisfied. We expect that whenever $P_{\nu_e\to\nu_e}\le e^{-1}$ for $E_{\nu_e}\approx 50$ MeV, the neutrino-induced event contributions should be similar to those listed in Table III for $P_{\nu_e\to\nu_e}=0$.

V. DISCUSSION AND CONCLUSION

The main effect of neutrino flavor mixing is to increase the number of $O(\nu_e,e^-)F$ induced events in both the KII and IMB detectors. This is readily apparent in Table III. In fact, $\delta N(\nu+e)\approx 1$ and 2, whereas $\delta N(\nu_e+O)\approx 25$ and 52 for the KII and IMB detectors, respectively. A substantial increase in the number of events induced by $O(\nu_e,e^-)F$ would signify the presence of neutrino flavor mixing, as well as give us some hint as to the ν_x energy spectrum. In fact, $^{16}{\rm O}(\nu_e,e^-)^{16}{\rm F}$ is the only process which can allow water Čerenkov detectors to probe the ν_μ and/or ν_τ neutrino-sphere temperatures.

Because we only have crude approximations for the neutrino energy spectra, our estimates for the relative contributions from individual neutrino interaction processes are more reliable than the calculated absolute numbers of individual events. We define the ratio of the number of $O(\nu_e,e^-)F$ induced events to that of $p(\bar\nu_e,e^+)n$ induced events to be f. We find that f increases from 1.66% and 1.55% without neutrino flavor mixing to 7.58% and 13.08% with full conversion of ν_x into ν_e for the KII and IMB detectors, respectively.

Identifying which neutrino-induced events are due to neutrino flavor-mixing effects is difficult. However, this task is facilitated by the different energy and angular distribution characteristics of events induced by different neutrino interaction processes. As explained previously, the neutrino-electron scattering induced events are rather insensitive to neutrino flavor mixing. Our subsequent analysis will, therefore, concentrate on the $O(\nu_e,e^-)F$ induced events.

We first note that the main product of $O(\nu_e,e^-)F$ is ^{16}F, which has no particle-bound states and decays to ^{15}O by proton emission almost spontaneously. The species ^{15}O then β^+ decays to ^{15}N (stable) with a half-life of 124 s. The emitted proton is not detectable in the current water Čerenkov detectors, while the emitted positron has a maximum energy well below the detection thresholds of both the KII and IMB detectors. We must conclude, therefore, that oscillation-induced events cannot be identified by the subsequent decay of ^{16}F.

The only hope for a clear neutrino flavor-mixing signature seems to be the backward-peaked electron angular distribution for $O(\nu_e,e^-)F$ induced events. Since neutrino-electron scattering induced events are sharply forward peaked, they are easily discriminated from $O(\nu_e,e^-)F$ induced events. Therefore we shall study the angular distribution for the combined $p(\bar\nu_e,e^+)n$ and $O(\nu_e,e^-)F$ induced events only.

In the case of full neutrino flavor conversion, the angular distribution for these two events combined is given by

$$P(\phi)\approx 0.5-0.076\cos\phi \tag{14a}$$

for the KII detector and

$$P(\phi)\approx 0.501-0.091\cos\phi-0.003\cos^2\phi \tag{14b}$$

for the IMB detector. If there were no neutrino flavor mixing, the angular distribution in both detectors should be approximately given by Eq. (1). We can distinguish these two cases as follows. Suppose we have N_0 events induced by $p(\bar\nu_e,e^+)n$ and $O(\nu_e,e^-)F$ in total. The difference in the number of events with $\cos\phi<0$ between these two cases will be $\Delta N\approx 0.012N_0$ and $0.020N_0$ for the KII and IMB detectors, respectively. Assuming no neutrino flavor mixing, there would be $N\approx 0.502N_0$ events with $\cos\phi<0$. To detect a statistically significant difference between the cases with and without neutrino flavor conversion, we must have $\Delta N>\sqrt{N}$. This implies that we must have a total of roughly 3486 and 1255 events induced by $p(\bar\nu_e,e^+)n$ and $O(\nu_e,e^-)F$ in the KII and IMB detectors, respectively, to give an unambiguous verdict on oscillations. Unfortunately, neither detector can satisfy this condition. The expected number of combined events is 454 in the KII detector and 510 in the IMB detector for a galactic supernova 10 kpc away (see Table III). However, if we assume that the SK detector is just an enlarged version of the KII detector, then the number of events will be approximately 15 times larger ($M_{\rm H_2O}=32$ kton for the SK detector), and the above condition is easily satisfied. Clearly, the tendency to obtain more backward-peaked events in a detector when significant neutrino flavor transformation is present is the signature of neutrino oscillations which we sought.

At this point, we feel that a few words on the angular resolution of the SK detector are in order. For the detection of neutrino transformations, all we require is that the detector be able to measure whether $\cos\phi<0$ or $\cos\phi>0$. However, it is always helpful to have the best angular resolution possible. With the increased number of neutrino-electron scattering events, SK can point back to a galactic supernova with an accuracy of 2.8° [5]. Once the direction of the supernova is found, an angular resolution of about 30° is already suitable for our analysis of neutrino transformation. This level of accuracy in angular resolution was achieved in the detection of SN 1987A neutrinos [6]. This precision in angular resolution will certainly exist in the future water detectors even if there

is no improvement in the angular resolution after KII is upgraded to SK.

We also want to comment on the effect of more realistic neutrino energy spectra on our above analyses. Numerical supernova models tend to give fewer high energy neutrinos than the neutrino energy spectra in Eq. (10) would give [9]. The spectra in Eq. (10) are fitted to match the peaks of the distributions found in numerical models. This feature of the neutrino energy spectra will indeed have influence on the calculation of neutrino signals in the detector. The effect of the neutrino energy spectra comes into our above analyses through the electron angular distribution and the absolute number of events in the detector. Because the electron angular distribution for ν_e absorption on oxygen is a superposition of contributions from neutrinos with various energies, the choice of neutrino energy spectra will not make too much difference in the angular distribution as long as the peaks of the spectra match those of the realistic spectra well enough. The positron angular distribution for $\bar{\nu}_e$ absorption on a proton is almost independent of the neutrino energy spectra. In deriving the numbers in the condition $\delta N > \sqrt{N}$ for seeing the signature of neutrino flavor mixing, we have only used the angular distributions and the ratio of the number of $O(\nu_e,e^-)F$ induced events to that of $p(\bar{\nu}_e,e^+)n$ induced events. The effect of neutrino energy spectrum uncertainty is reduced when we take the ratio of the numbers of events. Therefore the neutrino energy spectra only affect the prediction of the total number of events in the detector significantly. We could have scaled the number of events in KII from SN 1987A to predict the number of events in SK from a galactic supernova without making assumptions about the neutrino energy spectra. And this would predict at least a total of $11\times25\times15=4125$ events in SK (the factor 25 comes from the neutrino flux dependence on the distance to the supernova, and the factor 15 comes from the mass of water), still satisfying the derived condition $N_0 > 3486$.

Finally, we want to comment on the time-of-flight delay effects on supernova neutrino signals in the water Čerenkov detectors due to a finite neutrino mass. Because significant neutrino flavor conversion in supernovas may occur if neutrinos have mass, we feel that a consistent analysis of neutrino signals should include both effects of neutrino flavor mixing and time-of-flight delay due to a finite neutrino mass. According to the seesaw model and the nonadiabatic solution to the solar neutrino problem, ν_e and ν_μ have negligible masses [11] and suffer essentially no time-of-flight delay effects for a distance of 10 kpc. Only ν_τ would be massive enough to cause such effects in these models. (We warn that these models may not, however, correspond to physical reality.) Possible time-of-flight delay effects can only be observed in the forward-peaked scattering induced events, and these effects do not affect our above conclusions regarding the signature of neutrino flavor mixing. Of course, we have only discussed neutrino-induced events from the thermal emission phase. As for the ν_e from the neutronization phase, they will have been converted into ν_τ in the supernova and will propagate to the detector in this flavor state. Not only will these neutrinos be less likely to be detected due to the characteristically small scattering cross section with electrons, but they may also suffer a time-of-flight delay due to their heavier mass. A time-of-flight delay will cause these scattering induced events to be correspondingly dispersed in time, which makes the neutrino-induced events from the neutronization phase even more difficult to identify [22].

In conclusion, we find that the number of $O(\nu_e,e^-)F$ induced events in water Čerenkov detectors is very sensitive to neutrino flavor mixing in supernovas. If the SK detector is in full operation when the next galactic supernova explodes, the unique neutrino energy-dependent backward-peaked angular distribution of these events in principle allows an observable signature of supernova neutrino flavor mixing.

ACKNOWLEDGMENTS

We want to thank R. Mayle and J. R. Wilson for providing us with the density profiles from their supernova code. Y.-Z. Qian thanks the Institute for Nuclear Theory at University of Washington, Seattle for the opportunity to present an earlier version of this work at the supernova workshop in February 1992. He also acknowledges discussions with W. C. Haxton and J. Pantaleone. This work was supported by NSF Grant No. PHY-9121623, Calspace Grant No. CS-56-91, and IGPP Grant No. LLNL 93-02.

[1] G. M. Fuller, R. W. Mayle, J. R. Wilson, and D. N. Schramm, Astrophys. J. **322**, 795 (1987).

[2] G. M. Fuller, R. W. Mayle, B. S. Meyer, and J. R. Wilson, Astrophys. J. **389**, 517 (1992); G. M. Fuller, Phys. Rep. **227**, 149 (1993).

[3] J. Arafune, M. Fukugita, T. Yanagida, and M. Yoshimura, Phys. Rev. Lett. **59**, 1864 (1987); S. P. Rosen, Phys. Rev. D **37**, 1682 (1988). A brief review on this subject can be found in T. K. Kuo and J. Pantaleone, Rev. Mod. Phys. **61**, 937 (1989).

[4] T. K. Kuo and J. Pantaleone, Phys. Rev. D **37**, 298 (1988).

[5] A. Burrows, D. Klein, and R. Gandhi, Phys. Rev. D **45**, 3361 (1992); Nucl. Phys. **B31**, 408 (1993).

[6] K. S. Hirata *et al.*, Phys. Rev. Lett. **58**, 1490 (1987); R. M. Bionta *et al.*, *ibid.* **58**, 1494 (1987).

[7] W. C. Haxton, Phys. Rev. D **36**, 2283 (1987).

[8] H. A. Bethe, in *Highlights of Modern Astrophysics,* edited by S. L. Shapiro and S. A. Teukolsky (Wiley, New York, 1986).

[9] A. S. Burrows, in *Supernovae,* edited by A. G. Petschek (Springer-Verlag, New York, 1990); R. Mayle and J. R. Wilson, Astrophys. J. **334**, 909 (1988); R. Mayle, J. R. Wilson, and D. N. Schramm, *ibid.* **318**, 288 (1987); R. Mayle and J. R. Wilson, Phys. Rep. **227**, 97 (1993).

[10] J. N. Bahcall, *Neutrino Astrophysics* (Cambridge University Press, New York, 1989).

[11] H. A. Bethe and J. N. Bahcall, Phys. Rev. D **44**, 2962 (1991).
[12] GALLEX Collaboration, P. Anselmann *et al.*, Phys. Lett. B **285**, 390 (1992).
[13] S. A. Bludman, D. C. Kennedy, and P. G. Langacker, Nucl. Phys. **B374**, 373 (1992).
[14] S. Dimopoulos, L. J. Hall, and S. Raby, Phys. Rev. D **47**, R3697 (1993).
[15] E. L. Wright *et al.*, Astrophys. J. **396**, L13 (1992); R. K. Schaefer and Q. Shafi, Nature (London) **359**, 199 (1992); A. van Dalen and R. K. Schaefer, Astrophys. J. **398**, 33 (1992).
[16] Y.-Z. Qian, G. M. Fuller, R. Mayle, G. J. Mathews, J. R. Wilson, and S. E. Woosley, Phys. Rev. Lett. **71**, 1965 (1993).
[17] See G. Sigl and G. Raffelt, Nucl. Phys. **B406**, 423 (1993); S. Samuel, Phys. Rev. D **48**, 1462 (1993); G. M. Fuller, R. Mayle, J. R. Wilson, and D. N. Schramm, Astrophys. J. **322**, 795 (1987), for a discussion of neutrino effective masses in hot relativistic plasmas. There are no neutral current exchange contributions to effective mass differences for ν_μ and ν_τ since the number fluxes of ν_μ and ν_τ are identical to those for $\bar{\nu}_\mu$ and $\bar{\nu}_\tau$. Feynman diagrams for the lepton exchange processes discussed here are given by M. J. Savage, R. A. Malaney, and G. M. Fuller, *ibid.* **368**, 1 (1991).
[18] S. J. Parke and T. P. Walker, Phys. Rev. Lett. **57**, 2322 (1986); W. C. Haxton, Phys. Rev. D **36**, 2283 (1987).
[19] L. A. Ahrens *et al.*, Phys. Rev. D **31**, 2732 (1985); L. S. Durkin *et al.*, Phys. Rev. Lett. **61**, 1811 (1988); G. Zacek *et al.*, Phys. Rev. D **34**, 2621 (1986).
[20] The density profile in the envelope is essentially the presupernova profile. In this paper, we have adopted the presupernova density profile for the progenitor of SN 1987A. For a detailed description, see S. E. Woosley, P. A. Pinto, and T. A. Weaver, Proc. Astron. Soc. Austr. **7** (4), 355 (1989).
[21] D. Kiełczewska, Phys. Rev. D **41**, 2967 (1990).
[22] H. Minakata and H. Nunokawa, Phys. Rev. D **41**, 2976 (1990).